The Spacecraft SHM Experiment, Part 2: Integration, Challenges and Early Ground Science

Derek T. Doyle[1], Sue Lee[2], Joy Stein[3], Ben Cooper[4], Matthew Campisi[5]

Air Force Research Laboratories, Space Vehicles Directorate, Kirtland AFB, NM, 87117

and

Dr. Seth Kessler[6]
Metis Design Corporation, Boston, MA, 02114

The Spacecraft Structural Health Monitoring experiment began development in 2013-2014 for integration onto two separate flight experiments. Last year's publication focused on the development and preliminary testing for setting operational and science objective. This year the hardware has been integrated and ground measurements on the STP-H5 payload have begun. The goal for this hardware is identify the capability of this type of technology to enable greater insight into the structural status of a critical system or component. Integration also allowed researchers to identify secondary challenges facing the transition of such technologies and initiate a series of lessons learned to be applied to the second payload starting later in 2015. Integrated hardware has been used to monitor the assembly of the spacecraft and capture the integration steps of additional payloads. This paper will showcase the results and approaches for going through integration and current capabilities of the experiment to track the assembly process and the operational limitation given the equipment setup.

[1] Spacecraft SHM PI, Space Vehicles Directorate, 3550 Aberdeen Ave. SE, and AIAA Professional Member.
[2] Spacecraft SHM PM, Space Vehicles Directorate, 3550 Aberdeen Ave. SE, AIAA Non-Member.
[3] Associate Engineer, Space Vehicles Directorate, 3550 Aberdeen Ave. SE, AIAA Non-Member.
[4] ATA-A Intern, Space Vehicles Directorate, 3550 Aberdeen Ave. SE, AIAA Non-Member.
[5] AFRL Intern, Space Vehicles Directorate, 3550 Aberdeen Ave. SE, AIAA Non-Member.
[6] President/CEO, Metis Design Corporation, 205 Portland St., AIAA Non-Member.

I. Introduction

Structural Health Monitoring (SHM) has been integrated and began its ground measurements on the Space Test Program – Houston 5 (STP-H5) to monitor the assembly of the spacecraft and capture the integration steps of additional payloads. The goal for this hardware is identifying the capabilities of this technology to enable greater insight into the structural status of a critical system or component. Having the SHM system fully integrated and functioning on STP-H5 was the first step to gathering our ground science and allowed researchers to identify secondary challenges facing the transition of such technologies and initiate a series of lessons learned to be applied to the second payload starting later in 2015.

Commercial-Off-The-Shelf (COTS) solutions for SHM systems currently exist in different configuration strategies. One approach is to utilize a centralized Data Acquisition (DAQ) system to collect measurements from 'N' sensors distributed across the platform where the number of sensors, N, drives the design space of the centralized box in terms of power and volume required as well as resulting thermal loads. An alternate approach is modular distributed monitoring units where the central hub that starts the chain provides interface needs and is a bit more defined in terms of overall Size, Weight, and Power (SWaP). The difference being that each sensing unit of 'N' units now has a set amount of minimum requirements necessary to function as an individual unit on the chain. While this may increase total power and parts required it also minimizes the heat density by distributing the load across the structure and allowing for less signal noise due to less wire length. The chosen unit implements a fully digital SHM solution with the MD7-Pro system that is composed of 3 core elements: an Accumulation Node for remote data concentration and diagnostic processing, an Acquisition Node for distributed signal digitization, and analog sensor bases that mate with both types of nodes. Each element of the MD7-Pro system is networked on an 8-wire serial bus that carries command, data download, node synchronization and power. Benefits of this distributed infrastructure approach include higher fidelity data through digitizing sensor signals at the point of measurement, reduced computational burden through local signal processing and feature reduction, and overall minimal mass through the consolidation of cables and elimination of bulky off-the-shelf hardware.

The Accumulation Node is the first element placed at the front of any MD7-Pro bus. Measuring 60 x 40 x 5 mm with a mass of 20 g, the fundamental role of the Accumulation Node is to serve as an interface between the SHM network and the platform being monitored. It accepts 28VDC to distribute power for up to 100 daisy-chained nodes in a MD7-Pro network, along with relaying commands, facilitating synchronization, and storage of the resulting data. It can be programmed to run autonomously, communicate over Ethernet, or accommodate flexible provisions for other wired and wireless protocol. In addition, the Accumulation Node offers 8 analog and 8 digital acquisition channels (up to 16-bit 1MHz) and boasts 64GB of static memory. A powerful FPGA with an ARM core processor can be programmed to execute embedded diagnostic algorithms.

The MD7-Pro system can be efficiently expanded by daisy-chaining Acquisition Nodes. Measuring 50 x 40 x 5 mm with a mass of 15 g, the Acquisition Node is a direct replacement for traditional instrumentation such as rack-mounted oscilloscopes and function generators, enabling distributed data acquisition and signal processing. Each Acquisition Node provides a 20 Vpp 20 MSample/sec arbitrary function generator, 6 independent 12-bit channels of up to 50 MSamples/sec with programmable gain up to 500 or attenuation down to 1/500 in addition to 8 multiplexed 16-bit channels that share up to 1 MSamples/sec and 2 Gbit of DDR3 memory. The nodes are potted in urethane to provide resistance to moisture, chemicals, flame and shock loading, and have been designed to pass aerospace EMI standards. The Acquisition Nodes are capable of synchronously facilitating high sampling rate damage detection methods (guided wave, acoustic emission, and frequency response) while collecting multiple pre-conditioned differential voltage sensor signals (strain, temperature, acceleration, etc).

Both MD7-Pro nodes can accept a large range of appropriately configured sensor bases, which not only provide a mounting interface to the structure, but provide a physical connection to the external analog and/or digital sensors being monitored. Traditional SHM methods require dense sensor meshes to precisely resolve the position of damage, however this drives up system weight and complexity. Thus, in addition to customer specified custom configurations, MDC has patented a standard PZT beam forming array package that mates with the MD7-Pro Acquisition Node to facilitate both active and passive structural sonar scans. The Structural Sonar Array can indicate damage event coordinates using a novel sensor design along with an innovative algorithm with minimal information about the material or structure. From a single node position, a probability of damage map can be generated in response stiffness changes detected by an active guided wave scan, or due to the passively captured acoustic

response from an impact event. Results from multiple nodes can be combined synchronously and/or asynchronously to enhance sensitivity and resolution.

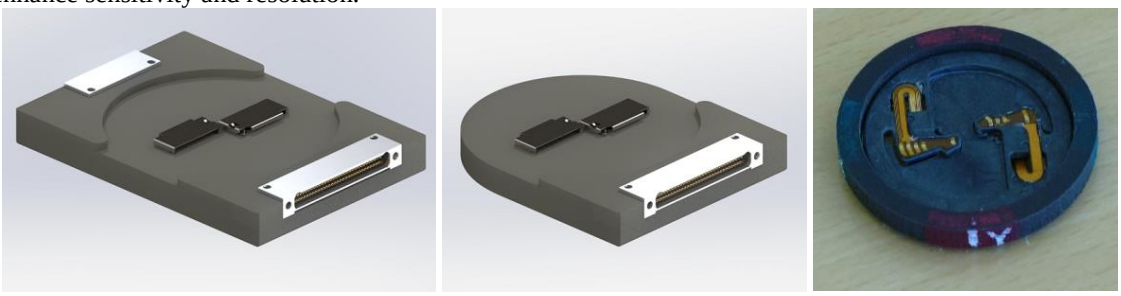

Figure 1 Basic Components of MD7-Pro SHM hardware showing (left to right) accumulation node, acquisition node and structural sonar array

Additional hardware can be attached to the acquisition nodes through an interface cable that breaks out a third wire set to accommodate analog and digital signals. They will be used on both flights with accommodating signal conditioning boards to monitor various voltage output sensors (accelerometers, shock, acoustic pressure, etc.). The configuration for STP-H5 can be seen in the following graphic.

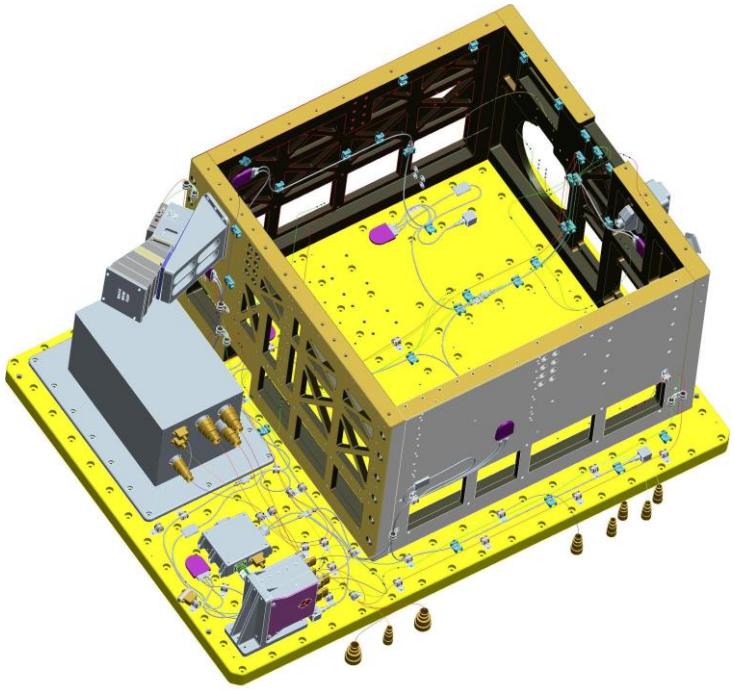

Figure 2 STP-H5 showing SHM system integrated layout across the bus

A. STP-H5 Mission Overview

The Space Test Program – Houston 5 (STP-H5) is a DoD Space Test Program payload that is currently slated to launch as part of the SpaceX 10 Mission in 2016. STP-H5 is attached to an Express Pallet (ExPA) and will attach to the International Space Station's ELC-1 (Express Logistics Carrier). The spacecraft SHM experiment was proposed to this mission to serve as a risk reduction experiment for future missions with higher operational demands. This mission would allow us to observe integration challenges that come with working on relevant systems and the utility/areas needing improvement of the current state of the art technology. SHM began its first phase of installation in August 2014 on STP-H5's common structure which involved the installation of three Kistler 8395a triaxial accelerometers tuned to the specific sensing range of interest to NASA partners. Phase 2 of the installation consisted of the installation of 8 nodes supporting 56 Piezoelectric Wafer Active Sensors (PWAS), 12 internal accelerometers, and 30 temperature sensors and supporting cables. The installation required special press on tools as can be seen in

the figure below. Phase 3 of the installation consisted of the installation of the SHM Hub Box which houses the Accumulation Node, RS-422 chipset, power isolation electronics. Currently, we are conducting our ground science experiment which involves ultrasonic guided waves and accelerometer measurements. The scope of the ground measurements is to assess repeatability of measurements in a relatively stable environment and track the assembly of the spacecraft as new components are added. Additionally once STP-H5 is finished and system level testing begins, we will track any changes to the structures overall state during critical qualification testing and transport. Current results will be presented later in section III of this paper.

Figure 3 Press on tool used to install Sensor base to structure.

While half of this experiments mission is conducted over the 12 month integration period prior to launch, the remaining half is achieved on orbit. Measurements will be focused on monitoring the structure initially for any drastic changes that occurred during launch and the progression of any other changes over a 12-24 month period on orbit. Changes are likely to be seen from a variety of incidents and each must be well understood to evaluate this approach for future systems. The first possible source of change is from the state of the hardware monitoring the system. Degradation of epoxy bonds, sensor damage, node rotation causing contact loss with electrodes, solder joints cracking from thermal stresses, etc. are all possible events that may end the hardware experiment in the harsh environment of space. This change is easiest to spot as it results in significant sudden changes in sensing data in the form of reduced or no energy in measured waveforms. Another source is from the environment. Temperature drives acoustic properties in material as well as stiffness of certain interfaces. The EM environment may introduce noticeable signal noise in the system. Charge buildup may affect the reference axis of measured data. Radiation may depolarize piezos reducing their response to mechanical and electrical input. The final source of expected change is from alterations to the structures boundary conditions. Interface slips during thermal shifts from eclipse or even micrometeoroid impacts changing local geometric features of the structure will impart changes into the measured waves. These changes are likely to be very minor relative to the other two areas and more difficult to analyze.

B. GEO Flight Overview

We are still reviewing publication rules for this section and resulting decision will be in final paper – we plan to outline the test plan for the GEO flight, how to power during various testing stages to accommodate launch monitoring, and how appropriate accommodations need to be made for the testing during the AI&T phase.

II. Component Level Testing

Each mission requires hardware go through simulated environmental testing to ensure the system was assembled correctly and will survive the expected conditions. Different missions will have different levels of testing required. Some will require workmanship only while others will want proto-flight or loads with margin beyond planned loads. Some missions may only recommend component level testing to support planed system testing while others may not be able to perform a full system test requiring extensive component testing. Each of the SHM missions have conflicting test strategies resulting in redundant testing. Testing may be combined or swapped for the scenario with

the larger test 'envelope' but there is a risk of damaging the system during testing and losing the validation results or both payloads. The following sections highlight the current results of testing done to the SHM system hardware.

A. Structural Analysis

Assessing the likelihood of the SHM system to survive launch requires structural analysis of the primarily the hub box structure as an electronics box weighing in at nearly 0.72kg. The nodes are of little concern due to the 3 square inches of epoxy holding the 20 grams of mass and cable mounts restraining the cable harness. Even if the bond failed, the chain would be held to the structure. The box however cannot be dismissed. The hub is approximately 3.5"x3.5".1.5" with a mass of 0.5kg omitting internal electronics cards and can be represented by the following figure and the table after shows properties applied to the various parts within the structure.

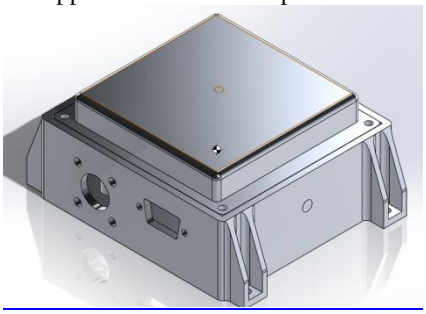

Figure 4 SHM Model used for structural analysis

Table 1 Material Properties of Model Parts

Property	Symbol	Units	6061-T6 Aluminum [2]	G10-FR4 Circuit Board [3]	18-8 Steel [3]
Ultimate Strength, Tensile	Ftu	psi	41900	40000	74700
Yield Strength, Tensile	Fty	psi	36000	19000	29700
Elastic Modulus	E	psi	10000000	2000000	30700000
Poisson's Ratio	M		.33	.11	
Density	r	lb/in^3	.098		.290
Specific Heat	C	BTU/lb F	.22		.120
Thermal Conductivity	K	W/in C	4.3	**.91/.014 ***	9.22
Thermal Expansion Coefficient	a	ppm/C			

The design geometry was developed in Solidworks and analyzed with the integrated finite element software Solidworks Simulation. Some non-critical features were eliminated (rounds, chamfers, etc) in order to reduce the computational requirements and mesh size.

Calculations were performed on all the mechanically fastened hardware using an excel spreadsheet that computes the axial and shear loads on each fastener in a pattern. These computed loads were then incorporated into the NSTS 08307 method for preloaded bolts. Fail safe analysis has been completed on all hardware to ensure there are no single points of failure present within the design. Analysis assumes a torque value of 7-10in-lb with a running torque of approximately 6in-lb. Results are summarized in Table 2.

Table 2 Hardware Analysis Summary [4-8]

Location	Fastener Material	Fastener Size	Safety Factor	NSTS 08307 Load/Bolt (lbf)	Allowable (lbf) /Bolt	MS	Failsafe MS
Hub to Baseplate	18-8 CRES	#6-32	2.0	494.3	679 (Ten) 511 (Shear)	+0.04	+0.03
Lid to	18-8	#6-32	2.0	490.1	679 (Ten)	+0.04	+0.04

Electronics Box	CRES				511 (Shear)		

The following load cases were applied based on input from the STP-H5 program [9].

Table 3 Load Cases from STP-H5 ICD

ICD Section	Load Case	X (g)	Y (g)	Z (g)
4.98	Ground Handling and Transportation	+/-5.0	+/-3.5	+/-3.5
4.99	Combined Load Factors	+/-22.4	+/-16.2	+/-16.2
4.100	Random Vibration*	+/-12.03	+/-12.03	+/-12.03
4.79	On-Orbit Loads**			
4.85	Load Spectrum**			

*Random Vibration loads can be assumed to be quasi-static using a 3-sigma approach which yields 12.03g in all directions. (4.01grms*3=12.03g)

**Because no loads are explicitly provided in the ICD, it is assumed that these loads fall well within the loads provided in Sections 4.98-4.100 and are therefore enveloped.

The analysis was simplified by realizing that the Combined Load Factors in Section 4.99 enveloped all the required load cases. All analysis in this report uses the +/-22.4g in x-direction, +/-16.2g y and z directions as it is the worst case loading that SHM will be subjected to during its lifetime.

The following dynamic loading (vibration) is examined to ensure a positive margin of safety exists for all load cases per SSP 52005.

The margin of safety calculation details are shown below with tables following showing results:

$$MS_U = \frac{P_U}{P_U FS_U} - 1 \quad (1)$$

$$MS_Y = \frac{P_Y}{P_Y FS_Y} - 1 \quad (2)$$

Where

$$MS_U = Margin\ of Safety\ against\ ultimate\ failure$$
$$MS_Y = Margin\ of\ Safety\ against\ material\ yield$$
$$P_U = Load\ (or\ stress) at\ which\ material\ failure\ will\ occur$$
$$P_Y = Load\ (or\ stress) at\ which\ material\ yielding\ will\ occur$$
$$FS_U = Ultimate\ factor\ of\ safety$$
$$FS_Y = Yield\ factor\ of\ safety$$

Table 4 Safety Factors from STP-H5

	Yield	Ultimate
Metallic Structure -Untested on orbit (analysis only)	1.25	2.0

Table 5 Calculated Margins of Safety

Component	Calculated Stress (psi)	Ultimate Stress (psi) (SF=2.0)	Yield Stress (psi) (SF=1.25)	MSu	MSy
Electronics Box Assembly	5428	10856	6875	2.86	4.24

Using the information provided in SSP 52005 and NASA-STD-5019, a part is low-risk when the maximum stress is less than 30% of the ultimate tensile allowable. If the stress is less than 16.7% of Ftu, then it is generally accepted that the part is good for infinite life. Finite element models of the SHM assembly were created to calculate the stresses and resonant frequencies of the components as a result of the quasi-static and dynamic (vibration) environments.

A finite element model of the SHM hub was developed in Solidworks Simulation 2013. The following image shows the model and the mesh. All loads were applied to the model at the center of mass. The launch axis is referred to as the x-axis in the ICD and correlates to the y-axis of the FEM. The model consisted of 16869 elements. It was assumed that the bolt hole edges common to the baseplate were fixed.

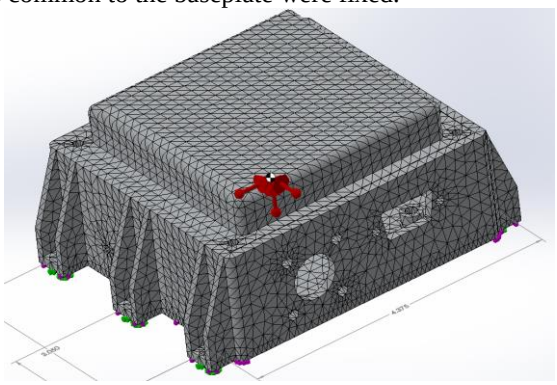

Figure 5 FEM created in Solidworks

All combination of the combined load factors were analyzed and resulting loads are shown as maximum predicted stress in the next figure.

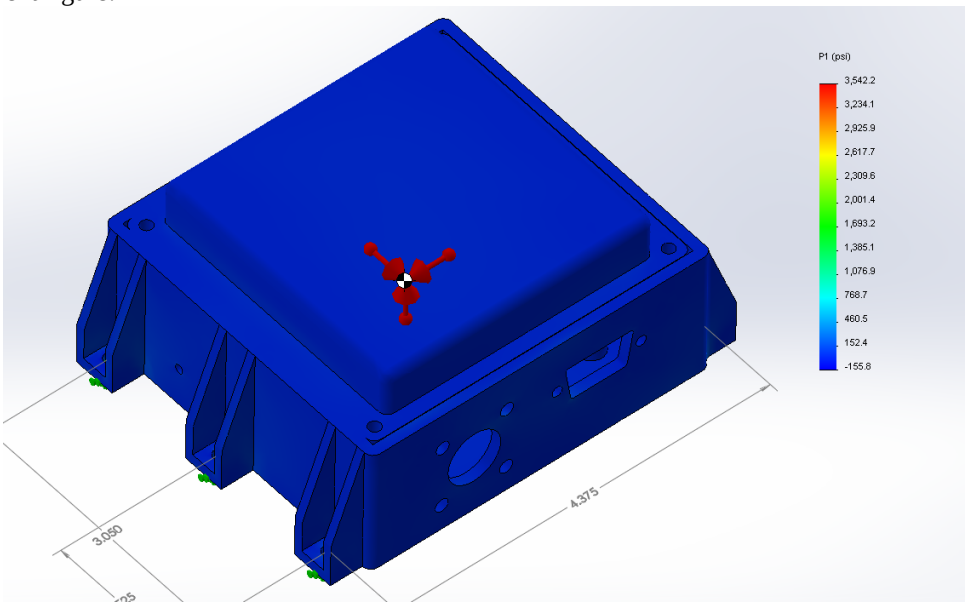

Figure 6 Static FEM Results--Stress (SF=1) Max stress=3110.6psi

The fundamental frequencies were estimated using a modal analysis with fixed restraints at the edge of bolt holes common to the baseplate and are summarized as follows.

Table 6 Modal Results

Mode	Frequency (Hz)
1	3137.3
2	3306.8

3	3799.2
4	4125.8
5	4467.3

Solidworks Simulation provides the ability to complete linear dynamic analysis. The same model that was used for the quasi-static load cases was used to do the shock analysis, however the restraint applied was different. Because it's assumed that there could be some flexing in the joint between the baseplate and the box of SHM, the box was fixed on the face common to the bolts. This changed the results slightly from the assumption used in the quasi-static case. The load applied was in the launch direction per the ICD. The predicted maximum stress was 1895psi and the result of the model is shown next.

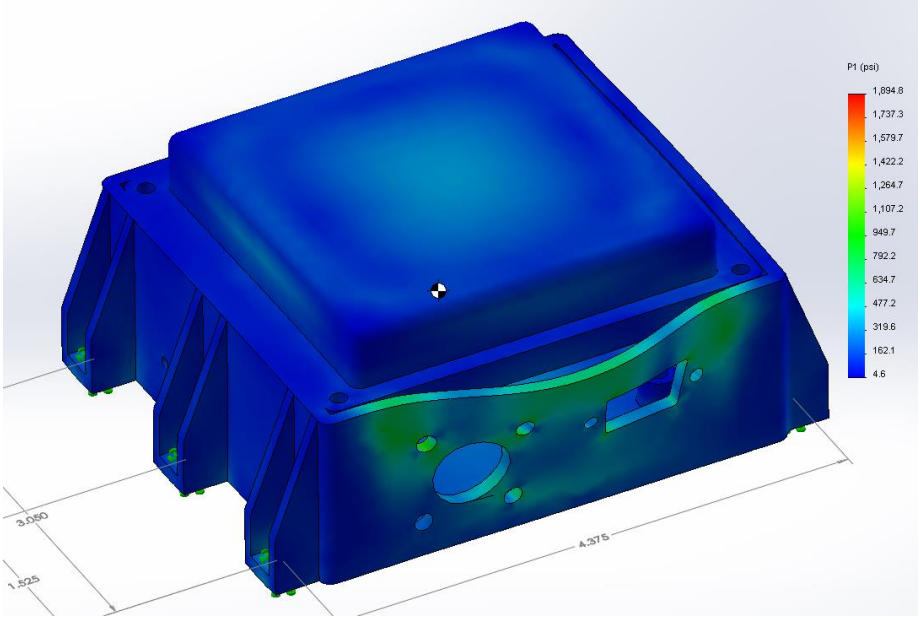

Figure 7 Results of Shock Response Analysis

Dynamic testing was performed at the Aerospace Engineering Facility (AEF), building 595 on Kirtland Air Force Base on December 5, 2014. The assembled SHM hub was bolted to an adapter plate and a node was attached per the flight procedures. The adapter plate was then bolted to the shaker head. After the z-axis (launch) axis was vibrated, everything was dismantled, the shaker was rotated 90 degrees and the adapter plate and SHM assembly was re-bolted to a slip table for the final two axes. This setup utilized a previous lid design that has since been modified to accommodate a more recently added DC/DC isolator card but analytical results are still within the expected range and all are well out of any range of concern (<150Hz).

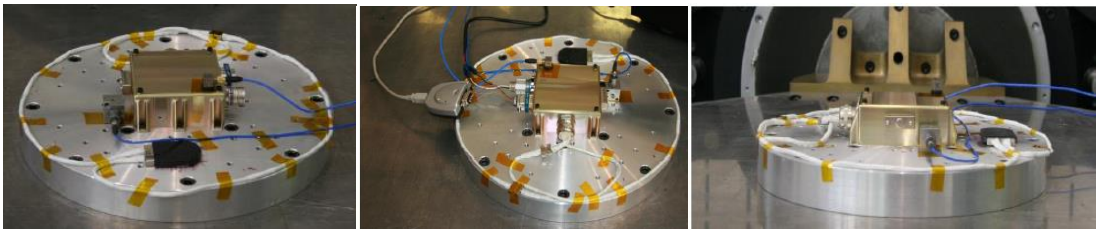
Figure 8 Vibe configurations (Left-Right): z-axis, y-axis, x-axis

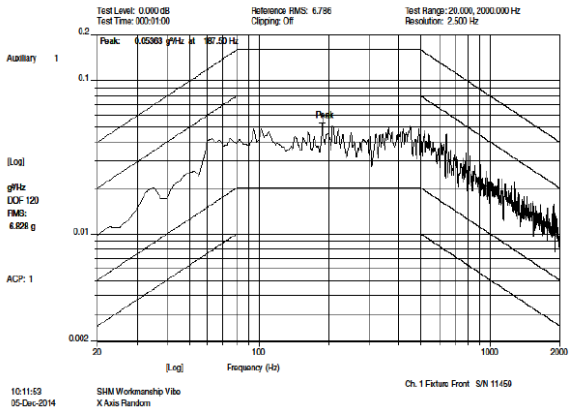

Figure 9 X-Random x-axis

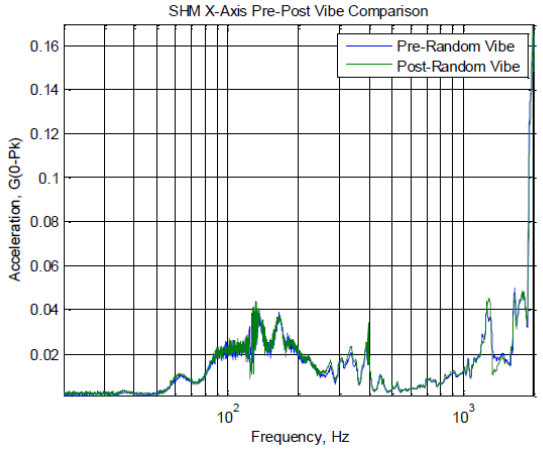

Figure 10 Sine sweep x-axis

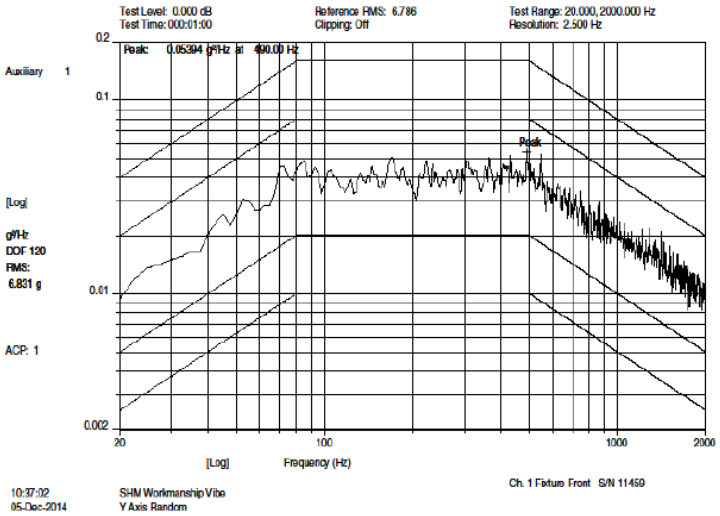

Figure 11 Random y-axis

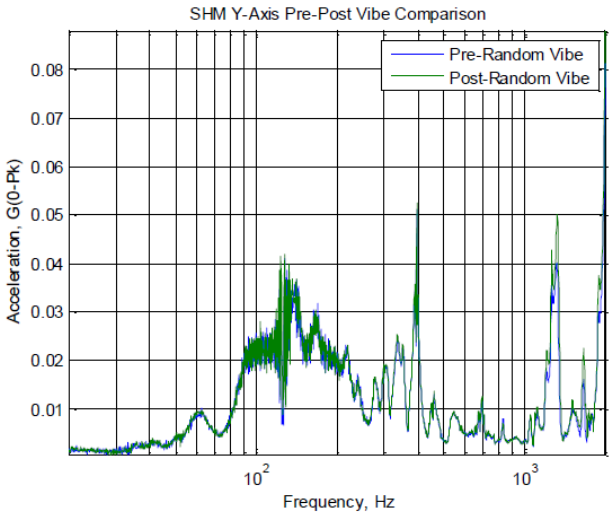

Figure 12 Sine sweep y-axis

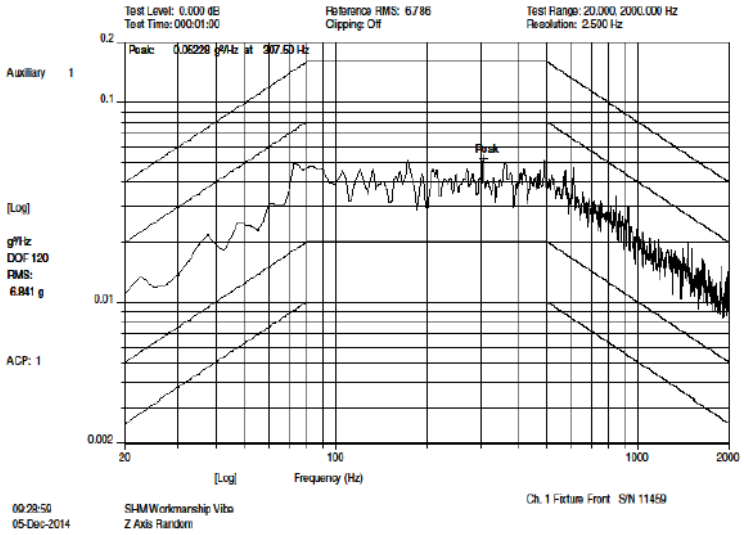

Figure 13 Random z-axis

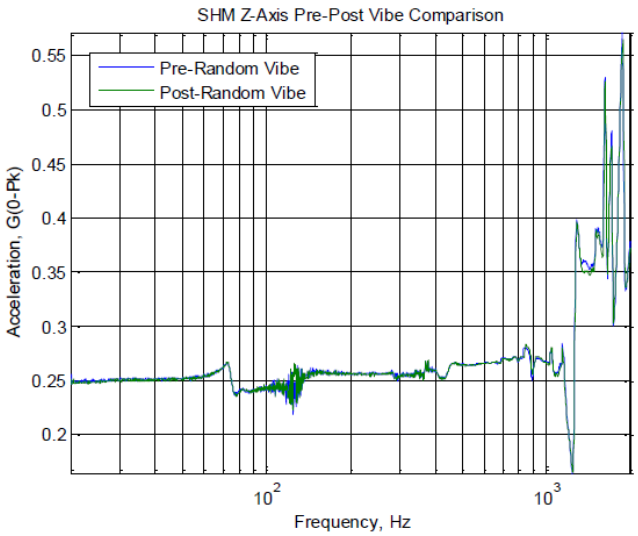

Figure 14 Sine sweep z axis

The test data show a first fundamental frequency at 1503 Hz. It should be noted that due to the size of the box and it's stiffness it was difficult to capture the fundamental modes. There were no significant changes in any axis when comparing the pre and post random sine sweep data. The minor peaks observed below 1000Hz are trivial with respect to the later peaks which capture the modes of interest.

The measured mass of SHM is 1.29 pounds. While this is a large percentage change (55% delta from what was modeled), this is acceptable because the actual change is approximately 5 ounces. A revised load was added to the critical load case to verify the previous analysis.

The loads were revised by the difference in mass from the model and the as-built assembly, or 0.91/1.29=1.55. The maximum stress increased from 3310psi to 4965.5psi or 1.5 times. The margins listed in Table 5 are somewhat reduced, but still positive as shown below.

Table 7 Expected Loads on Revised Structure

Component	Calculated Stress (psi)	Ultimate Stress (psi) (SF=2.0)	Yield Stress (psi) (SF=1.25)	MSu	MSy
Electronics Box Assembly (as built mass)	4965.5	9931	6206.9	3.22	4.80

The STP-H5 ICD requires various analysis be performed for crew induced loading. No crew involvement is expected for STP-H5; the only analysis performed was for inadvertent or loading where the crew was expected to be moving to another area of the station.

The requirements in Ref 8 Table 4.10-1 Extravehicular Activity Induced Loads require analysis of EVA Kick-Off, Push-Off of a Tethered Crew Member or an inadvertent kickload to any of the faces of a payload. The affected area is assumed to be a circular area with a 3" diameter incurring a 200lbf load. Because of the size of SHM, the only area on which this can occur is the lid.

An additional case is noted as an "inadvertent kick, bump" over an area with a 0.5" diameter circular area. Again, because of the design of the box, the only location that this could occur is on the lid. This load was assumed to be the same 200lbf load as the Kick-Off or Push-Off load. The lid was classically analyzed as a simply supported plate with bending per Reference 7, Table 26. The lid was analyzed as Case 1b; the side was analyzed as Case 9a. The results listed below include a safety factor of 2.

Table 8 Margins for Kickloads and Bump

Component	Case	Resulting Stress (psi)	Material Allowable (psi)	MS (w/SF=2)
Box Lid	Kickload	1468	41900	+13.27
Box Lid	Bump	5110.8	41900	+3.01

B. Thermal Vacuum Testing

A component level thermal vacuum test should be performed on flight hardware to ensure the workmanship of the assembled product including soldered interfaces and other mated component under operational and survival thermal limits. These values may come from the hardware build of material specifications or from a detailed thermal analysis of the system in the relevant environment. Most vendor hardware specifies both limits for maximum operating and storage limits to prevent damage. When defining a flight program concept of operations (CONOPS) and constraints it should be considered that the proposed limits may be less than what is stated by the specification guidelines. The reason for this is that electronics heat up quickly in vacuum with no other mode of cooling but through conduction. This limitation may require one to operate an FPGA at lower capacity to reduce the thermal build up. While it may be safe to operate up to 50C, for example, a particular component turned on at 45C may quickly exceed 60C due to thermal waste from current draw. Early predictions from modeling of the SHM hardware made it seem like a 15C delta would be standard for a hub or node drawing about 1W of current. However, final hardware proved to draw more quiescent current than planned. For this reason, an exploratory thermal vacuum test was developed to not only test the current expected thermal limits but also test the duration at which the hardware could safely operate before requiring shutdown. The specified minimum limits for SHM hardware is -65/-45C to 70/85C operational/survival. For STP-H5 the expected system limits are -20 to 40C but for a later GEO mission there is no known system limits and requirements are being driven by hardware specifications. Therefore researchers need to know what practical environmental limit the hardware can perform possible measurements given the rate of heat generated during operation.

One drawback of a distributed sensing system arises at this point when designing the test. Since each node contains electronics and generates its own heat to manage, which is primarily dumped into the base plate through the epoxy bond restricting its rotation from the sensor patch, then we must account for these units in a test. However to test a node on a system other than its final operational platform is to remove it from the batch of final flight units as a node cannot be permanently installed on two different systems. Additionally, since the central hub houses a DC/DC converter to isolate the SHM system from the space vehicles power source, the required transformer for the system produces heat from the inefficiency of the unit. SHM's DC/DC converter is 90% efficient. One way to get around this is to test one node and one hub box with a heater patch attached to the box lid to simulate the wasted heat produced by the remaining nodes not on the chain. While this is not a 1:1 comparison, it will give insight into the expected heat loads building up on the hub box. So if the hub requires 100mA and each node requires 70mA of quiescent power than the isolation brick is producing 0.1*(28V*(0.1A+N*0.070A)) of waste heat in Watts. For STP-H5 the total expected test-on power will be about 28*(0.1+0.070*8) =18.48W while the GEO flight will be about 49W. The thermal test plate contains the hub and node and generates 5.6W on its own meaning it has to simulate the difference. The central hub box will therefore have an added 1.2W or 4.3W to manage in the form of waste heat from the DC/DC converter managing the systems total power draw.

Ideally, this input would be placed directly into the transformers housed within the DC/DC card, however flight assembly prohibits the addition of the patch buried within the box between the card and the recessed pocket in the lid as seen in the following figure. Perhaps one approach may have been to apply a heater patch to a separate aluminum plate matching the profile for the DC/DC card housing and then apply that to the lid with a thermal gap material to attempt to match the bottleneck that the DC/DC card has inside the box to the lid, however this may not have been accurate as well given the thermal path between the transformers and the aluminum housing of the case of the DC/DC card is complex to accurately model as well. Instead, a 115V 2"x2" patch heater with resistance of 655 ohms was applied to the lid with an accompanying thermocouple to monitor the lid temperature. The goal is merely to identify the range of expected thermal gradients within the box from the lid to the base plate with minimal risk to the flight unit through complex modifications.

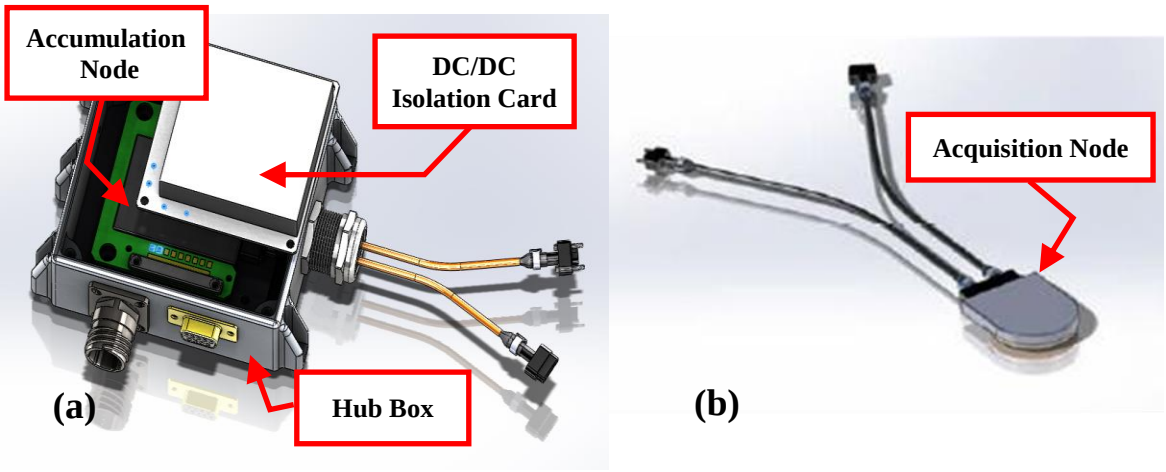

Figure 15 Assembly blowup of SHM Hub (a) and acquisition node with attached V-cable (b)

Once the system was mounted to an adapter plate with cold plate set to 20C the system was powered on to run just the hub resulting in 0.14A of current draw on a 28V source. Kirchhoff's law was used to derive the necessary voltage of the patch heater to simulate the same input power in the box. The patch was run at 50V and allowed to reach equilibrium. An additional test was then run where the patch heater was left off and just the hub ran allowing the system to reach equilibrium. The resulting thermal paths of the thermocouples is shown below.

Final results will be presented in final paper. At time of submission, tvac testing is on day 2 of a 2 week test. There will be results for how the system performs at operational limits and the duration of test that can be supported.

C. EMI/EMC Testing

This process is still under development and will be presented in the final version

III. Integration and Ground Science

A. Ultrasonic Testing

Guided wave measurements were taken of the structure as the sensor were installed to check for installation workmanship and assess the overall capability of the current sensor arrangement. Of critical importance was first verifying that hardware was not fluctuating in the cleanroom which fluctuates by about 5-10 degrees at most. Any noticeable variations would drive the threshold values that analysis approaches would need to define 'damage' or some form of change. The following figure shows the system to be very repeatable in time and frequency domains.

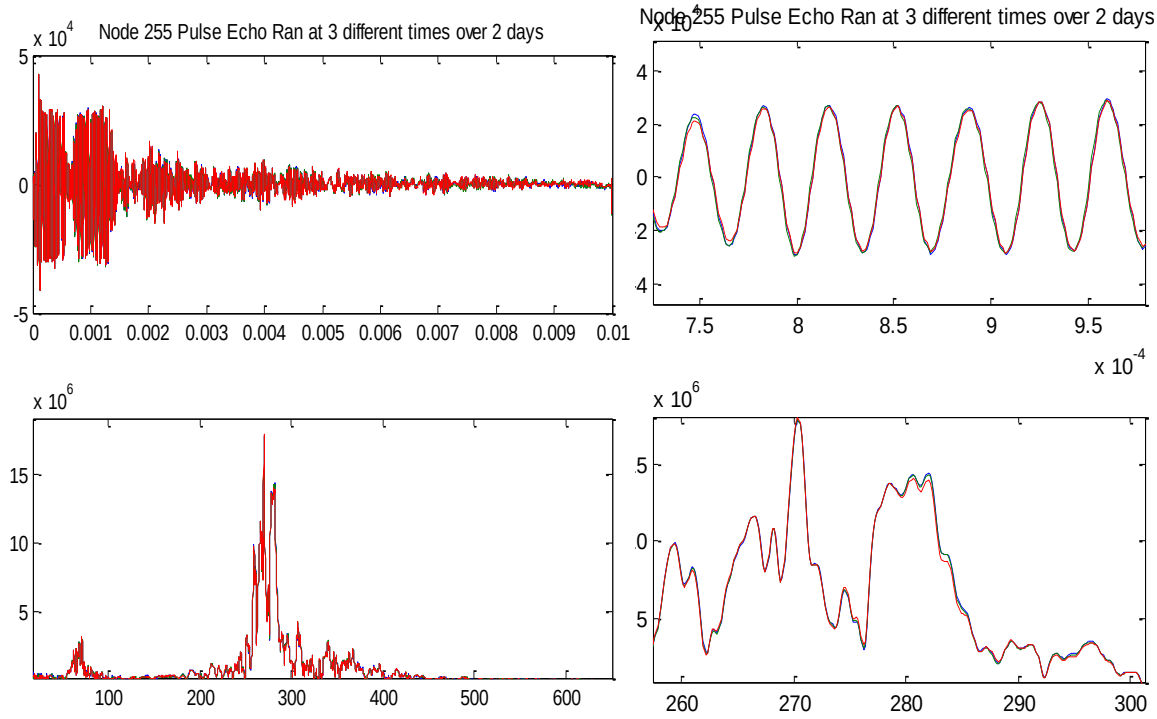

Figure 16 Pulse echo measurement from node 255, whole data set (left) and a zoomed in region (right)

Additionally, authors had to check for energy transfer from the base plate to the bunker walls which rest on top of the base plate. It was initially believed that the wall thickness and feature patterns made the transfer from one to the other unlikely to take place. However, results can be seen in the next figure where waveforms are recorded on a bunker wall with a node on the base exciting.

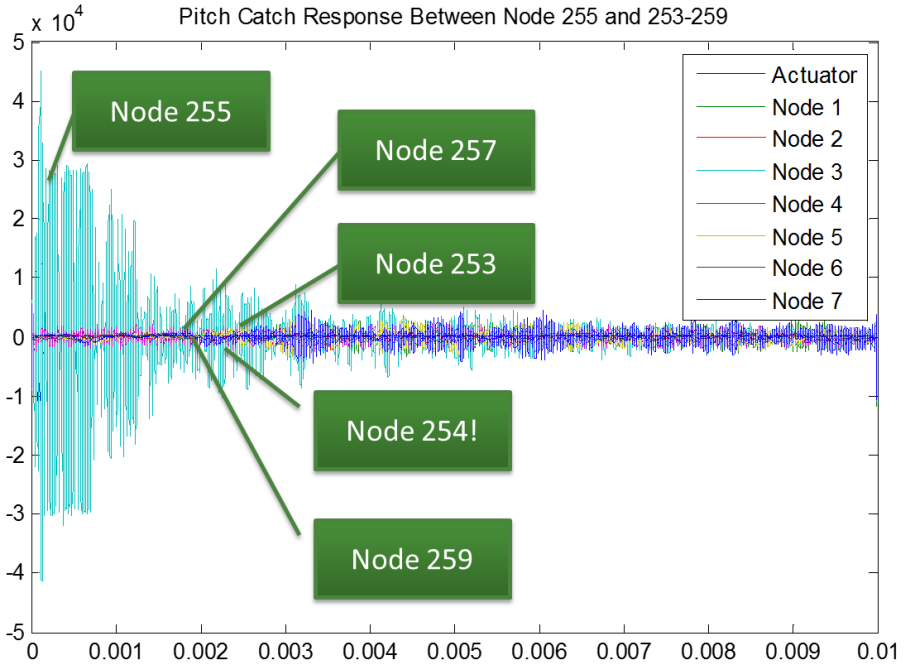

Figure 17 Pitch Catch measurement using one channel from each node to show the distance a wave propagates and the energy through the plate interfaces to the bunker.

B. Tri-axial Accelerometer Preliminary Results

The SHM experiment on STP-H5 has been configured to accommodate 3 separate tri-axial accelerometers placed on the base plate of the structure in an orthogonal arrangement so as to assess the dynamic environment and body modes of the hosting plate of the experimental mounting fixture on the International Space Station truss. NASA expressed interest in this particular measurement for future experimenters that may have sensitive optical hardware. The SHM nodes are capable measuring these accelerations (or other voltage output devices) utilizing modular components and different cable configuration. Accelerometers are interfaced to nodes via a 'W-Cable' and an accompanying signal conditioner block to maximize the measurement window of interest. For STP-H5 the desired sensing range was defined at +/- 0.2 g's by potential future payloads based on best guesses for the current expected range. As of this date the actual environment of this location is unknown through physical measurements. The final integrated hardware was tested to assess the sensitivity and noise in the sensor and SHM hardware chain. A 100 Hz sampling was taken of the three sensors for 10 seconds. The raw data was processed using the equations below for vibration and temperature data provided by the Kistler specifications for the sensor. The STP-H5 base plate with various other payloads is seen in the following figure. The base rests on a pallet mounted on 4 hard wheels. The room utilizes a raised floor structure to allow access to infrastructure and the clean room fame mounts to this raised room structure.

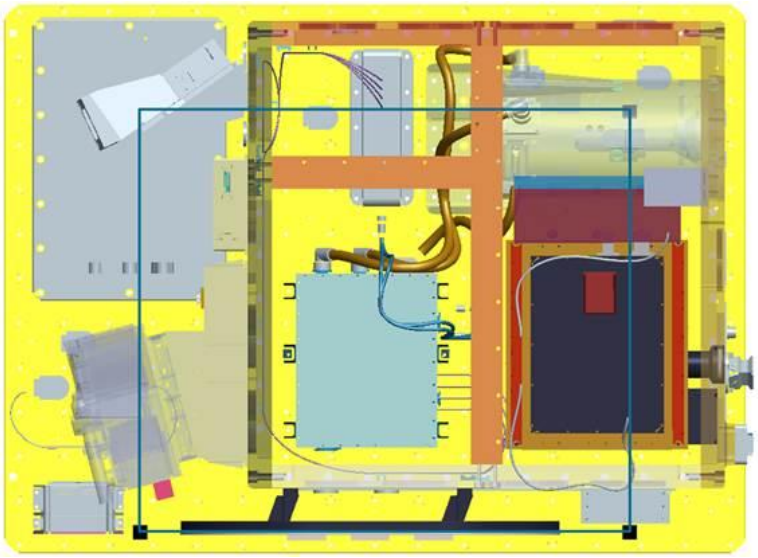

Figure 18 STP-H5 with accelerometer locations indicated by the 3 black squares aligned with the blue rectangle outline where the 'base' is 30.38" and 'height' is 26.4" of separation between accelerometer mounting stud centers.

$$a = \frac{[ch1\ ch2\ ch3] - \left(\frac{R_{bit}}{2}\right)}{2.5 * R_{bit}} \tag{3}$$

$$T = \frac{\left(Ch4 * \frac{2500}{R_{bit}}\right) - 1187.28}{5.65} \tag{4}$$

Internal electronics control the output of the temperature and acceleration sensor within the tri-axial accelerometer where acceleration, a, is centered by defining the 0 axis as the center of the data acquisition resolution, R_{bit}, and normalized by 2.5 multiplication of the sensing resolution. Temperature is calibrated by the vendor with the weighted values used to obtain the correct value (with 9^{o} F of possible range error)

A sampling of the data shows that the x and y channels are approximately experiencing 0g's of acceleration which is to be expected with them being perpendicular to Earth's gravity. The z channel is pinned at 0.2 g's due to the desired sensing range being exceeded by the Earth's gravity. This conditioning allows for maximum resolution within the sensing window of interest. Temperature is scaled and plotted on the graph just to show the 9 degree variance within the sensor as mentioned in the hardware specifications, however the standard deviation only appears to be

approximately 3°F. The standard deviation for the measured acceleration in the clean room with ventilation fans running for the both x and y channels of all 3 sensors were all around 7.7e-4 g_{ms}.

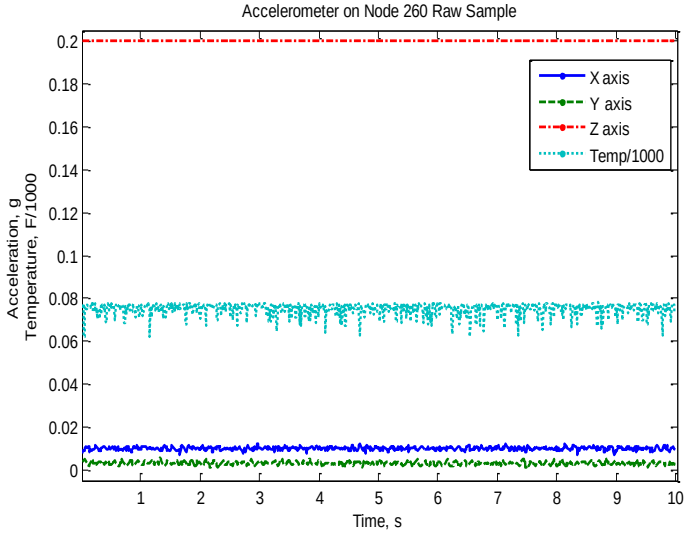

Figure 19 Raw data taken from node 260's connected triax showing 3 axis channels and the scaled temperature to fit the window

To test the response of the system to environmental input, technicians performed a tap test of approximately 4 beats per second as best guessed by the individual tapping. The 4th tap was executed with more force to flag in the raw response ideally. The resulting signal was measured and is shown below where standard deviation for temperature and the y-axis channel are about the same as the first test (4.2 degrees and 9.4e-4 g's) but the x-axis had a noticeable signal to it with deviation of 2.5e-3 g's.

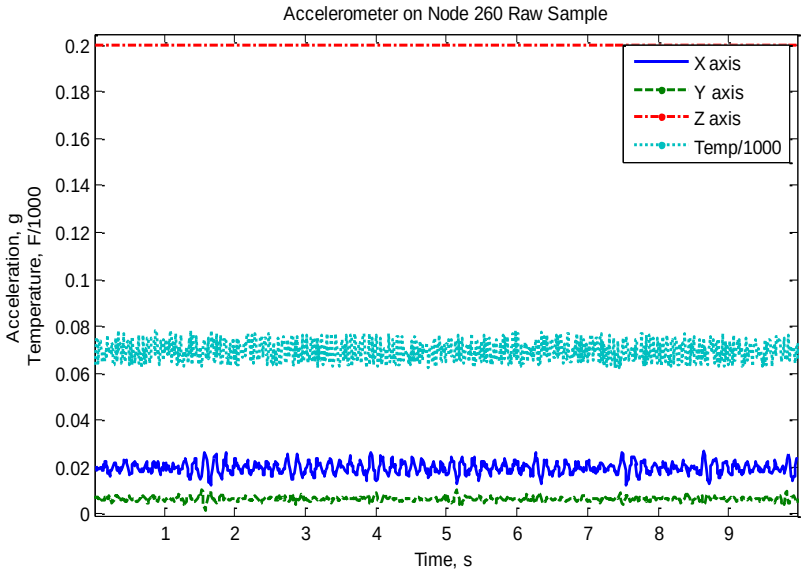

Figure 20 Raw data from a second test were technician tapping was done on sensor to ensure functionality

A power spectrum density was calculated for all sensors and channels using Matlab's pwelch function on the signal processing toolbox with no windowing or overlap as the input signals seem to be fairly consistent. The following 3 figures showcase the x and y axis data for different environmental stimuli in the lab when sampled at 100 Hz. The first graphic showcases the profiles present in the clean room when just the filtration fans are running. While slight amplitude variation is seen, the actual variation between accelerometers is trivial when compared to other forms of input. Of interest is that the oscillation on the floor from the ventilation system imparting a noticeable signal on the structure. Average acceleration can be approximated as g_{rms}, and is defined by the area under the curve. For a well-defined peak, this can be approximated by taking the square root of the product of the peak and base value. This

can't be done for the z-axis as it is oversaturated but the x and y axis channels all resulted in approximately 7e-4 g_{rms}. The only exception was the x axis measurement for node 257 that reported 1.2e-3 due to the other minor peaks that showed in the signal. At these levels it is more likely that the discrepancy may have something to do with the sensitivity of the specific sensor. To get perspective for how small these values are; if the current structure mass is estimated at 150kg and we apply the measured accelerations then we can approximate the vibration of the clean room imparting nearly 1.11N (0.25 lbf) to the x and y axis of the pallet that currently rests on wheels. The wheels likely have an impact of dampening the force from the floor.

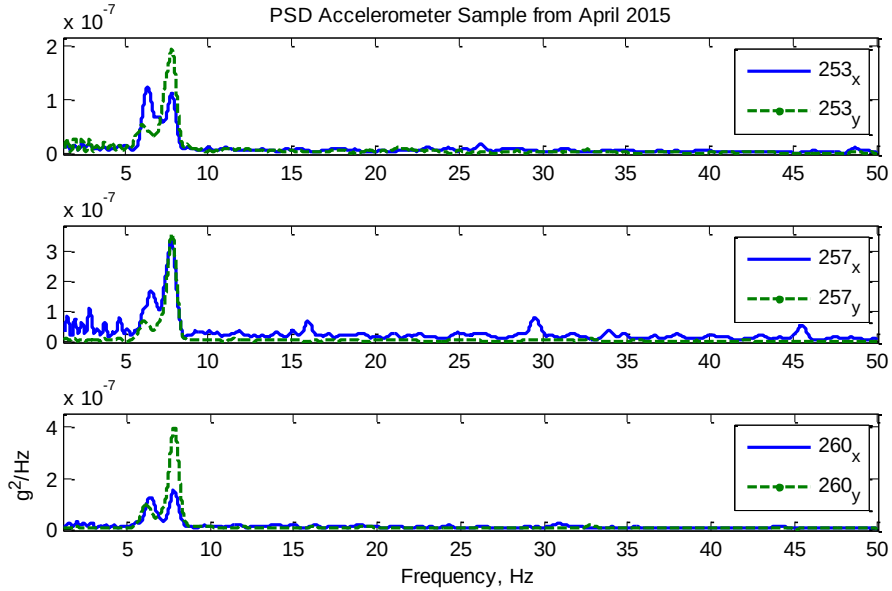

Figure 21 PSD of ambient room environmental loads on systems 3 triaxial accels

The raw data from the tap test shows a clear sinusoidal waveform in the x-axis that matches the expected trend from the technician. Ideally we would expect the sensors to be rigidly mounted to the structure so that the tapping on one sensor should show up on the others. If the mounting configuration of the accelerometer is dampened by either the fastener preload or the epoxy bond supporting it, then we may see less energy transferred to accelerometers further away. The below figure shows the PSD of the test and as expected the energy in the x-axis greatly exceeds the y-axis. On all 3 sensors the y-axis showed a 9.3e-4 to 9.7e-4 g_{rms}, or about 6.23N (1.4 lbf), while the x-axis all reported 2.2e-3 to 2.5e-3 g_{rms}, or about 14.68N (3.3 lbf). A quick literature search provided a study on finger tapping force from patients of various states of health and reported tapping forces between 1.12 and 6.7 lbf [1]. This merely verifies the approximate loads seem to be reasonable and readers should be reminded that the exact weight of the system under test is only approximated at this time for the purpose of assessing early performance of the sensing system.

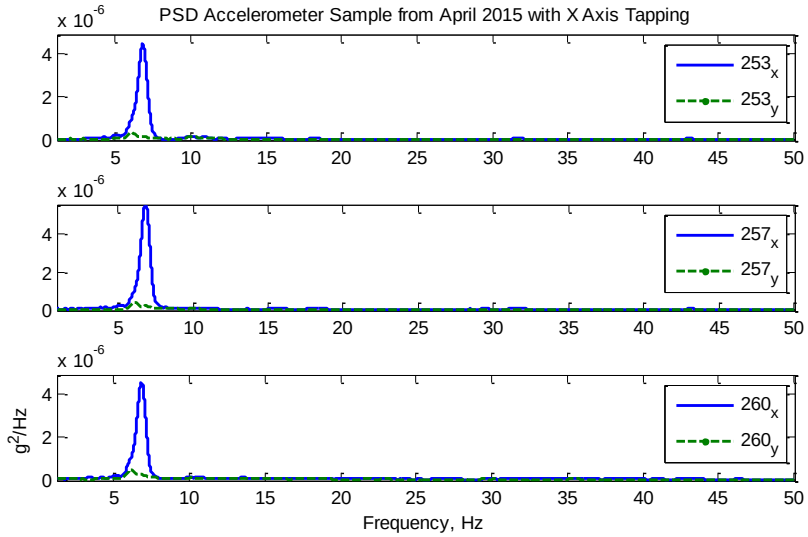

Figure 22 PSD of ambient room environmental loads on systems 3 triaxial accels and added technician tapping

On a follow up integration trip one month after the previous test, further build up had been performed and a new benchtop vacuum pump had been placed in the clean room and is left running constantly providing a new source of input into the clean room's floor. While to pump rotation is well beyond the 100 Hz previously monitored, a noticeable oscillation could be felt in the floor from it. A repeated sampling revealed new peaks in the measurements with stronger values than the earlier ambient room environment. The loads were still minimal with average forces between 5.75 and 8.45N (1.3 and 1.9 lbf) observed.

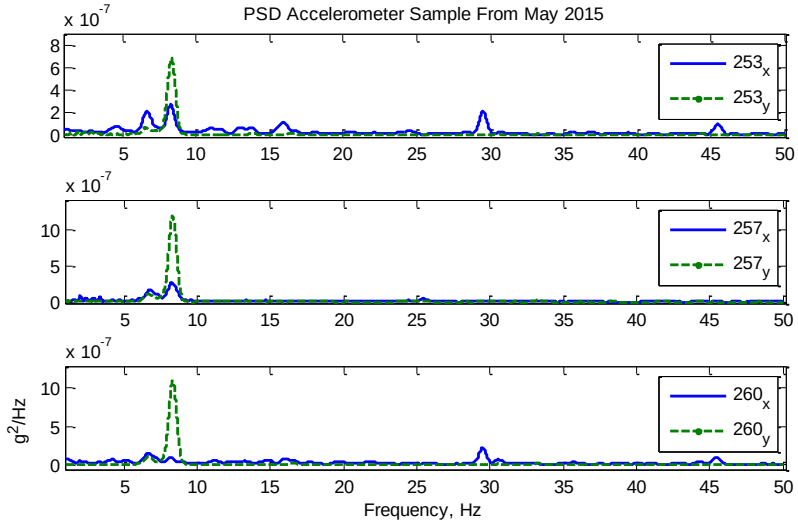

Figure 23 PSD of ambient room environmental loads on later trip with new hardware running in lab

Effort is going into making a GUI intended to be an interactive interface to compare two sets of triaxial accelerometer data. This could compare a baseline noise environment and the accelerations observed during a particular test or event. Similarly the comparison of similar operating conditions (active pumps or motors) during different time frames. The interface allows flexibility in viewing and probing data by allowing all or a few sensor channels to be plotted. The different accelerometer data can be filtered through the most common means (lowpass, highpass, bandpass, and notch) with some control over the filter shape. The spectrum (represented by PSD) is always visible in the left side along with the filtering options. In addition, the spectrum can be viewed in the main plot axes, as well as the original and filtered signals for individual accelerometers independently. Readers are encouraged to look into online available codes like 'ifilter' available on the mathworks site for assistance in

generating their own similar analytical GUIs. The current effort can be seen in the following figure showing the filtered data for the tap test done by the technician.

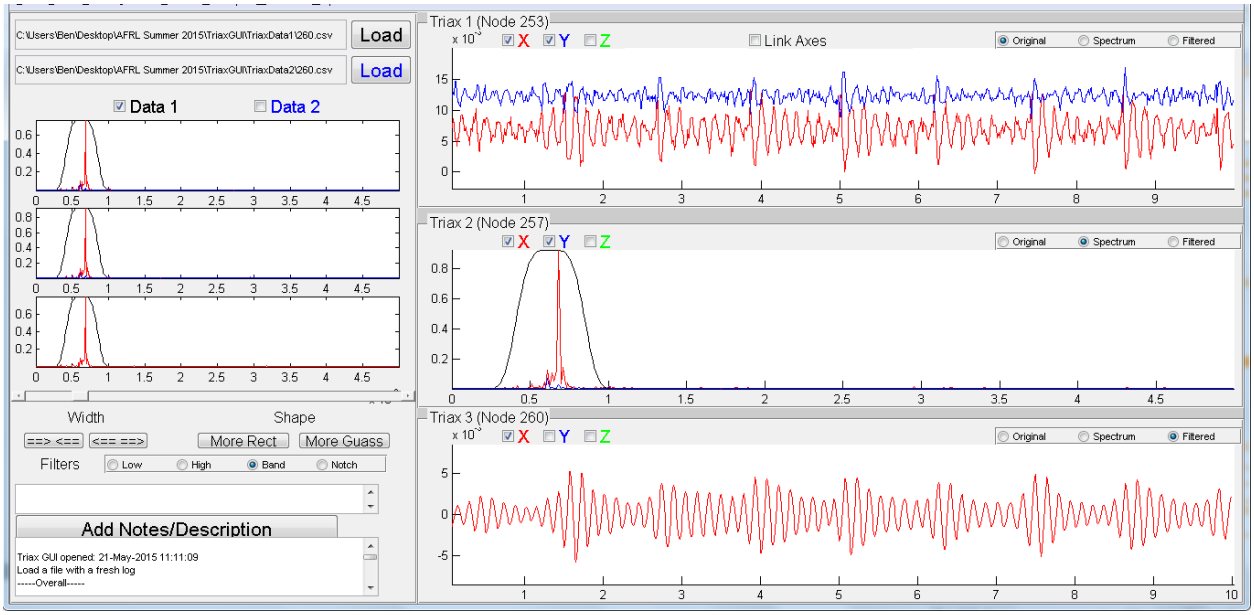

Figure 24 Interactive GUI for evaluating accelerometer data

An addition tool is being developed to manage the data and files of the SHM results from the Accumulation hub to aid in data collection and analysis. The tool will organize records to a designated location based on measurement header information. The tool is a graphical user interface developed in Matlab and utilizes Matlab structures to handle the data from the results files. The structure of the Matlab files makes it simple and less labor intensive for other Matlab programs to utilize and analyze the data by:

- Combining a single test or run files into a single .mat file (Matlab structure file).
- Storing all data and information stored in the .csv files into a well-documented and easy to navigate format.
- Creates a folder structure that makes it easy to navigate to the desired tests to retrieve the data.
- Improves and streamlines the processing and interfacing capabilities with other Matlab programs or GUIs that need the information.

Certain protocols for analysis tools will have to be put into place to ensure that the data maintains its integrity as slight software modifications are still being made. The GUI can be used to acquire and backup all of the data stored in the Results folder or any level of the testing down to a single test or run. The authors feel this is a critical task to properly preserve and make the resulting raw data readily available for other interested parties that may be interested in applying their own analytical techniques at later dates. Failure to implement such basic data management disciplines prior to the start of an experimental mission can result in lost, misplaced, or improperly categorized data requiring the exclusion of valuable data sets.

IV. Lessons Learned

Throughout the installation phases, SHM encountered a few hardware/software issues due to the fact that SHM did not have enough test time with the accelerometers to deliver a mature data acquisition system upfront, SHM was the first to receive and integrate the first edition of the latest COTS Metis hardware. With a strict schedule and new hardware, it challenged both the developer and user to get the hardware/software to its flight operational ready state, which involved troubleshooting hardware/software issues and determining when it was time to draw the line and accept a limited operational capability. Currently, the hardware is at 80% flight operation based on initial expectations and the software is at 90% flight operational status, which allows us to achieve 90% of our end goal. Being the first payload to integrate using first edition hardware has its own advantages and disadvantages. On one hand, earlier integration efforts are: less rushed and stressful, provide easiest accessibility, and allow for a long post

install period for additional testing or optimization. However, it also puts the greatest stress on the software development as hardware will often use up all available schedule buffers. Additionally, the early install required integration to be done in phases preventing full level component checkout. The fact that the system wasn't thoroughly tested as a whole before final integration was a moderate-risk that authors and the STP-H5's team were aware of and both agreed to activities that were put in place in case issues were encountered, and of course, they were

Still to Discuss: manufacturing errors, inability to do sensor optimization with real integration activities, etc.

V. Conclusion

Conclusions will be written in the final paper submission

Acknowledgments

Authors would like to thank Dr. Stargel at AFOSR who funded much of the preliminary research and algorithm developments that have been used to for the development of this experiment. Additional thanks to the Space Test Program (STP) in Houston that is sponsoring the integration/flight of this experiment. The SHM experiment will fly on two different systems. The first will be as part of the DoD Space Test Program's STP-H5 payload. STP-H5 is integrated and flown under the management and direction of DoD's Space Test Program. STP-H5 is attached to an ExPA (Express Pallet) and will attach to the International Space Station's ELC-1 (Express Logistics Carrier). Additional support from the LoadPath, LLC team during thermal vacuum tested was also critical for testing the hardware under vacuum.

References

1. Shima, K., Tamura, Y., Tsuji, T., Kandori, A., Yokoe, M., and Sakoda, S., " Estimation of Human Finger Tapping Forces Based on a Fingerpad-Stiffness Model," 31st Annual International Conference of the IEEE EMBS, 2009, accessed from http://www.bsys.hiroshima-u.ac.jp/pub/pdf/C/C_189.pdf on 6/1/2015.
2. Military Standarizations Handbook: Metallic Materials and Elements for Aerospace Vehicle Structures, MIL-HDBK-5E, Washington, DC, Department of Defense
3. www.matweb.com Online Materials Database
4. Payload Flight Equipment Requirements and Guidelines for Flight Safety-Critical Structures. SSP 52005. International Space Station Program. Revision C. December 18, 2002.
5. Criteria for Preloaded Bolts. NASA 08307. National Aeronautics and Space Administration. Revision A. July 6 1998.
6. Standard, Threaded Fasteners, Torque limits Criteria for Preloaded Bolts. MSFC-STD-468B. National Aeronautics and Space Administration. November 1992.
7. H-II Transfer Vehicle (HTV)/Space Test Program-Houston 4 (STP-H4) Interface Control Document. JHX-2011087. Revision NC. December 2 2011.
8. Roark's Formulas for Stress and Strain 6th Edition. Young, Warren C. McGraw Hill. 1989.
9. Space Test Program-Houston 4 (STP-H4) Internal Interface Control Document. DoD Space Test Program. April 2011.